

Emergence of geometric order from topological constraints in a three-dimensional Coulomb phase

Benjamin Canals¹

¹*Université Grenoble Alpes, CNRS, Grenoble INP, Institut NEEL, 38000 Grenoble, France*

(Dated: March 2, 2026)

The emergence of order and geometric limit shapes in a three-dimensional (3D) Coulomb phase subject to domain wall boundary conditions (DWBC) is investigated. While the arctic circle phenomenon—the spatial segregation of frozen and fluctuating degrees of freedom—is well-established in the two-dimensional six-vertex model (square ice), its extension to 3D remains largely unexplored. A cubic lattice model with Ising degrees of freedom living on the edges, whose ground state manifold is governed by a divergence-free (3-in/3-out) local constraint, is considered. In the bulk, this model realizes a classical spin liquid characterized by algebraic correlations and pinch-point singularities in reciprocal space. It is demonstrated that applying DWBC partially lifts the extensive ground state degeneracy, inducing long-range magnetic order in the thermodynamic limit. Despite this ordering, it is found that the system retains a fluctuating component that exhibits the signature of a Coulomb phase. Finally, by mapping the local vertex polarization density, compelling numerical support is provided for a 3D generalization of the arctic limit shape, bridging the gap between topological constraints and emergent geometry in higher dimensions.

Introduction.— The study of constrained statistical systems has revealed deep connections between local geometric rules and emergent macroscopic behavior. A paradigm of this physics is found in “spin ice” materials and their theoretical abstractions, known as Coulomb phases [1]. In these systems, the minimization of local energy leads to an extensive ground state degeneracy, where the absence of long-range order is accompanied by critical, algebraic correlations. These correlations are often signaled in reciprocal space by “pinch points,” a fingerprint of the underlying divergence-free gauge structure.

While the bulk properties of these phases are well understood, the imposition of specific boundary conditions can lead to striking phenomena. The interplay between local geometric constraints and macroscopic spatial inhomogeneity is most strikingly realized in the so-called “arctic circle” phenomenon. Originally coined in the combinatorics literature regarding random domino tilings on the Aztec diamond [2], this theorem describes the emergence of a sharp boundary separating a “frozen” ordered region from a “liquid” disordered interior. In the realm of condensed matter physics, an equivalent behavior arises in the two-dimensional six-vertex model (or square ice) [3] when subjected to domain wall boundary conditions (DWBC). While the bulk model represents a critical Coulomb phase, the specific imposition of DWBC—pioneered by Korepin in the context of the Quantum Inverse Scattering Method [4, 5]—breaks translational invariance and forces a spatial segregation of the degrees of freedom. The determination of the exact limit shape separating these phases has been achieved through various methods, ranging from variational principles on dimer models [6, 7] to exact calculations of the Emptiness Formation Probability (EFP) by Colomo and Pronko [8], and was recently confirmed experimentally [9].

These foundational results in two dimensions natu-

rally invite the question of whether such sharp geometric boundaries and induced order persist in three-dimensional Coulomb phases. In this paper, the generalization of the arctic circle concept to a 3D lattice model is addressed. Three specific questions are raised: first, can a marginal constraint, such as boundary conditions, induce true long-range order in a 3D disordered Coulomb phase? Second, if the system partially orders, what is the nature of the remaining fluctuations? And finally, does an emerging limit shape exist in 3D?

To answer these, a model constructed on a cubic graph is considered, which can be viewed as a corner-sharing lattice of octahedra—a natural 3D extension of the 2D corner-sharing tetrahedra found in square ice. The Ising degrees of freedom reside on the edges, interacting ferromagnetically to satisfy a divergence-free condition (three spins in, three spins out) at every vertex. The results show that DWBC indeed have a profound effect in 3D. By computing the order parameter scaling, it is demonstrated that the boundaries select a subset of the ground state manifold that supports long-range magnetic ordering. Furthermore, by subtracting this ordered background, it is revealed that the residual fluctuations still exhibit the pinch points characteristic of a Coulomb phase. Finally, by monitoring the spatial evolution of the local vertex polarization, strong numerical evidence is provided for the existence of a 3D limit surface, effectively generalizing the arctic circle phenomenon to a three-dimensional spin ice.

The Model and Ground State Manifold.— A cubic graph where Ising degrees of freedom, $\sigma = \pm 1$, are located on the edges is considered (see Fig. 1). The interactions are defined between nearest neighbors:

$$\mathcal{H} = -J \sum_{\langle i,j \rangle} \sigma_i \sigma_j \quad (1)$$

Each nearest neighbor pair, i.e., when two edges belong to the same vertex, interacts ferromagnetically, meaning that two oriented edges minimize their two-body interaction when they are head-to-tail. This can also be interpreted as a corner-sharing lattice of octahedra, analogous to how the 2D square ice model is interpreted as a corner-sharing lattice of tetrahedra.

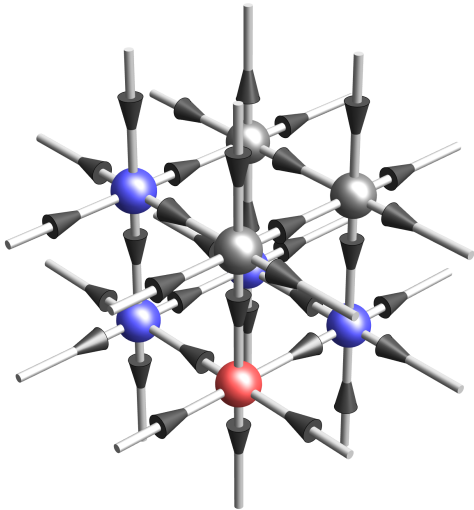


FIG. 1. The underlying graph of the model. Ising degrees of freedom live on the edges of the graph, such that any configuration maps onto an orientation of the edges. Spheres at the vertices depict the nature of the vertex: gray satisfies the ice rule (3-in/3-out), while blue and red indicate defects (2-in/4-out and 2-out/4-in, respectively). In the constrained ground state manifold, no 6-in or 6-out vertices appear.

On each unit cell (each octahedron), a minimal energy configuration corresponds to a divergence-free configuration: there must be three arrows pointing inwards and three outwards. Consequently, there are 20 allowed ground state configurations out of the $2^6 = 64$ possible configurations for each vertex. By mapping these arrows to a vector field \mathbf{F} defined on the edges of the lattice, this local constraint naturally translates into an emergent Gauss law, $\nabla \cdot \mathbf{F} = 0$.

It is possible to demonstrate that the ground state manifold is extensively degenerate. Consider a finite cubic cluster subject to open boundary conditions. It can be prepared in a fully polarized state before searching for loops of arrows (closed head-to-tail paths or open border to border head-to-tail paths). If such a loop is flipped, the divergence-free constraint is preserved by construction. Given that these loops proliferate, the ground state manifold possesses an extensive residual entropy. Therefore, the conditions for the realization of an Ising Coulomb phase are met [1]. One way to characterize this phase is to analyze the magnetic structure factor (see Eq. 3), which exhibits the well-known fingerprint of pinch points (see Fig. 2). In other words, the ground state mani-

fold is a disordered critical manifold, hosting algebraic correlations but no long-range order.

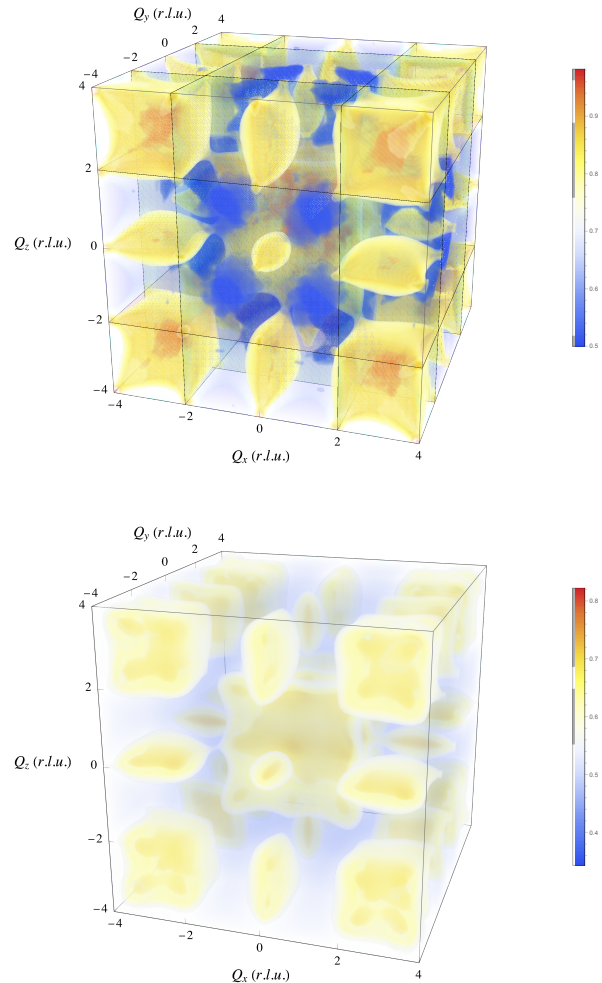


FIG. 2. (Up) Magnetic structure factor $S(\mathbf{q})$ of the ground state manifold of the model on a finite graph ($L = 21, N = 3L^2(L + 1)$) subject to open boundary conditions. It exhibits the fingerprints of a 3D Coulomb phase: a structured diffuse scattering with characteristic pinch points. These are the reciprocal space signatures of algebraic correlations (cut off in a finite system) related to the local divergence-free constraint [1]. The planes forming the Brillouin zone boundaries are visualized and indexed in reciprocal lattice units (r.l.u.). (Bottom) Structure factor of the spin fluctuations, $S_{\text{fluc}}(\mathbf{q})$, under domain wall boundary conditions (DWBC), obtained by subtracting the long range order. Despite the reduced spectral weight due to the frozen boundary, the persistence of clear pinch points confirms that the bulk interior remains in a fluctuating, divergence-free Coulomb phase.

Domain wall boundary conditions.— Domain wall boundary conditions (DWBC) are introduced to the finite cubic cluster. Unlike open (or periodic) boundaries which preserve the topological triviality of the bulk, the specific DWBC chosen here impose a global topologi-

cal charge imbalance on the system (see inset in fig.3). Specifically, the boundary spins are configured to enforce a net difference between incoming and outgoing flux. To satisfy this global constraint, the system must host a population of defects carrying magnetic charge (i.e., 2-in/4-out vertices). A crucial feature of the present model is that while the *net* topological charge is dictated by the boundaries, the individual charge carriers are **not pinned** to the surface. Instead, they represent *mobile* degrees of freedom that are free to diffuse into the bulk via local spin flips.

It is essential to emphasize the subtle nature of the thermodynamic limit, which hinges on two distinct constraints: the global boundary conditions and the magnetic charges they inject. Since the number of these topological charges scales with the surface area (L^2), their density relative to the total volume (L^3) vanishes as $1/L$. In this sense, these defects are thermodynamically marginal. However, the bulk physics remains strictly governed by the emergent Gauss law. It is the boundary conditions themselves that impose a macroscopic flux, forcing the field lines to traverse the entire sample over a typical length L . Furthermore, because the injected charges are not extreme defects (i.e., lacking all-in or all-out configurations), the flux lines that encounter them are not interrupted; they continue their trajectory. The resulting braided network of flux lines thus occupies an effective volume $L^2 \times L \propto L^3$, transforming a surface constraint into a true volumetric effect.

Note that, to properly explore this constrained manifold, a stochastic dynamics (a zero temperature monte carlo approach) is used; this dynamics must combine single spin flips (local updates) —allowing the injected charges to remain mobile—with loop flips (global updates), which are essential to sample the extended divergence-free fluctuations inherent to the bulk Coulomb phase [10].

Conceptually, the imposition of domain wall boundaries places this study within the broader lineage of limit shape problems in statistical mechanics. This approach parallels seminal investigations into the ferromagnetic Ising model subject to antagonistic boundary conditions, where the competition between surface tension and bulk entropy dictates the macroscopic geometry of phase separation. Following the principles of the Wulff construction [11] and its formalization by Dobrushin *et al.* [12], a global shape emerges from local rules. Crucially, within the ice manifold, this geometry is purely entropic. Since boundary-induced defects are thermodynamically marginal, the internal energy is almost surely uniform. Consequently, the minimization of free energy reduces strictly to the maximization of configurational entropy, selecting an arctic polytope (as detailed below) via an effective entropic surface tension.

Induced long range order.— To characterize the im-

print of domain wall boundary conditions on the ground state manifold, a global order parameter defined as the spatial average of the local magnetization magnitude was computed:

$$m = \frac{1}{N} \sum_i |\langle \sigma_i \rangle| \quad (2)$$

Given that the boundary conditions explicitly break translational invariance, this observable is particularly well-suited to detect the emergence of long-range order within a spatially heterogeneous structure. The evolution of this order parameter as a function of system size is presented in Fig. 3. The data demonstrates a convergence toward a non-zero value in the thermodynamic limit, providing clear evidence of symmetry breaking. Consequently, the DWBC do not merely constrain the edges but effectively restrict the system to a subset of the ground state manifold; this subset preserves, on average, the same type of topological charge as the macroscopic vertex defined by the applied boundary conditions.

In other words, the topological charge injected by the DWBC constitutes a marginal constraint. Specifically, for the 2-in/4-out DWBC, this constraint materializes through the injection of a marginal number of magnetic charges ($N_m \propto L^2$). However, in the thermodynamic limit, the induced long-range order manifests, surprisingly, as a macroscopic magnetic charge.

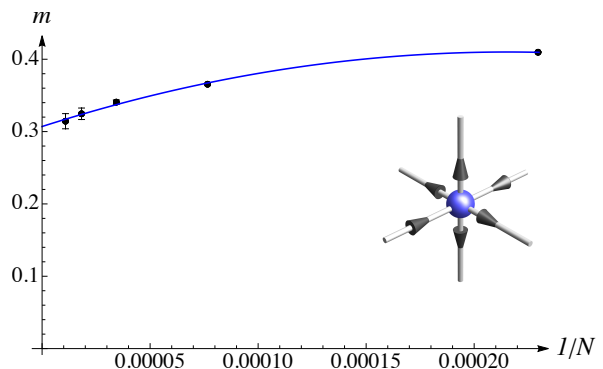


FIG. 3. Evolution of the spatially averaged order parameter m as a function of the inverse system size $1/N$ ($N = 3L^2(L+1)$), for $L = 11, 16, 21, 26, 31$. The solid line is a polynomial fit. The non-vanishing value at the intercept ($1/N \rightarrow 0$) indicates that the order persists in the thermodynamic limit, confirming that the boundary conditions select a specific subset of the ground state manifold. The inset schematically represents the global boundary conditions as a single effective vertex. Each of its six edges corresponds to an entire boundary plane of the simulated cubic volume: an inward-pointing arrow indicates that all spins on that specific macroscopic face are fixed to point uniformly into the bulk, defining the global 2-in/4-out configuration. Note that the topological constraint of the DWBC takes here the form of a marginal magnetic charge injection ($N_m = L^2$). This is to be contrasted with the usual DWBC applied in 2d, which are charge neutral.

Nature of fluctuations.— The observation that the induced long-range order is spatially heterogeneous and does not saturate the magnetization ($m < 1$) implies that significant fluctuating degrees of freedom persist within the subset of the ground state manifold selected by the DWBC. To characterize this residual disordered component, the magnetic structure factor $S(\mathbf{q})$ of the fluctuating sector was computed. The definition involving spin components perpendicular to the scattering vector \mathbf{q} is employed, a choice motivated here by the lattice geometry. Since the magnetic moments reside on the edges of the cubic cells, spins belonging to different sublattices are mutually orthogonal, rendering their direct scalar product null. The use of the transverse projection circumvents this geometric orthogonality, allowing the relevant correlations between distinct spin components to be captured:

$$S(\mathbf{q}) = \frac{1}{N} \sum_{i,j} e^{i\mathbf{q}\cdot(\mathbf{r}_i - \mathbf{r}_j)} \langle \delta\mathbf{S}_i^\perp \cdot \delta\mathbf{S}_j^\perp \rangle, \quad (3)$$

where N is the number of sites and $\delta\mathbf{S}_i^\perp$ denotes the projection of the local spin fluctuation $\delta\mathbf{S}_i = \mathbf{S}_i - \langle \mathbf{S}_i \rangle$ onto the plane perpendicular to \mathbf{q} . The resulting scattering profile exhibits sharp pinch points in reciprocal space (see Fig. 2, bottom). These singular features are the hallmark of algebraic correlations, demonstrating that the boundary conditions do not fully freeze the system but instead preserve an extensive degeneracy. It is precisely this residual entropy, coupled with the local divergence-free constraint ($\nabla \cdot \mathbf{F}_{\text{fluctuating}} = 0$), that sustains a critical Coulomb phase within the fluctuating background.

The 3D arctic limit shape.— In the two-dimensional six-vertex model, the selection of a ground state subset by domain wall boundary conditions (DWBC) manifests as a spatial phase separation bounded by the celebrated arctic circle limit shape. To investigate the emergence of an analogous boundary in three dimensions, the local vertex polarization, which serves as an order parameter quantifying the density of the frozen ferroelectric phase, is analyzed. The spatial decay of this polarization mirrors the behavior observed in the square ice model. By defining the interface as an iso-surface of the polarization density (i.e., fixing a specific density threshold), a macroscopic boundary is delineated whose convex envelope exhibits a geometry consistent with a 3D generalization of the arctic circle to an “arctic polytope,” as illustrated in Fig. 4.

However, a rigorous confirmation of this limit shape would require demonstrating that the polarization profile converges to a non-analytic step function in the thermodynamic limit. In two dimensions, this was first explicitly proven in ref. [2] but also via the exact solution of the EFP[8], which is a very efficient tool to numerically reveal the abrupt transition between the frozen and liquid phases. In the present 3D study, the absence of a generalization of the EFP, combined with the limitations

on accessible system sizes, prevents a similar definitive demonstration. Consequently, while the numerical results strongly suggest the emergence of a sharp interface, distinguishing this scenario from a smooth crossover remains a challenge for future theoretical developments.

This spatial phase separation finds a natural theoretical description in terms of “magnetic fragmentation,” a concept introduced by Brooks-Bartlett *et al.* [13] based on the Helmholtz-Hodge decomposition. In this framework, the local Ising spin degrees of freedom effectively fractionate into two independent sectors: a “divergence-full” part carrying the magnetic charge (static order) and a “divergence-free” part supporting the Coulomb phase correlations. Crucially, however, the breaking of translational invariance by the DWBC imposes a unique twist on this scenario. Unlike conventional fragmentation scenarios where the two fluids coexist uniformly throughout the volume, the DWBC enforce a *spatially heterogeneous* fragmentation. This points toward a scenario of macroscopic topological segregation in the thermodynamic limit: the ordered, divergence-full component saturates the exterior, while the fluctuating, divergence-free channel is confined to the interior.

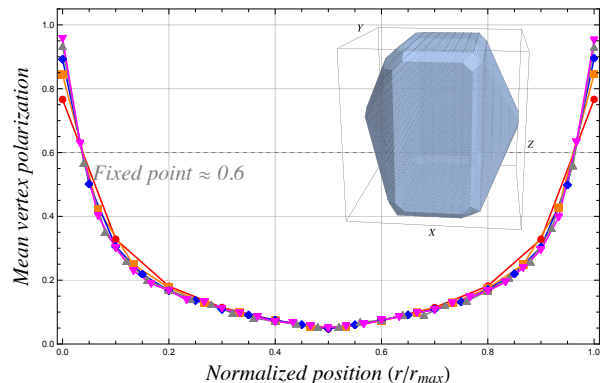


FIG. 4. Profile of the mean vertex polarization along the diagonal of the cube, for different sizes ($L = 11, 16, 21, 26, 31 - N = 3L^2(L + 1)$). In the inset, the convex hull of the mean vertex polarization is shown, with a chosen mean vertex value threshold = 0.1.

Conclusion and Outlook.— In summary, compelling numerical evidence is provided for an “arctic polytope” in three-dimensional spin ice, generalizing the celebrated arctic circle phenomenon. Despite injecting a marginal defect density ($N \propto L^2$), domain wall boundary conditions impose a global constraint via the emergent Gauss law. The resulting braided flux network drives a macroscopic segregation, offering a novel, spatially heterogeneous realization of 3D magnetic fragmentation into ordered and fluctuating Helmholtz-Hodge sectors.

The primary theoretical challenge is now to analytically derive this 3D limit surface. Experimentally, while boundary control in bulk crystals is elusive, emerging 3D

artificial spin ice platforms [14] could enable the engineering of specific topological constraints to directly visualize the arctic polytope.

Finally, this scenario places spin ice within the broader class of systems governed by entropic ordering, alongside hard-sphere crystallization [15], depletion [16], and critical Casimir forces [17, 18]. Macroscopic rigidity and geometry emerge here not from energetic bonds, but from the system’s relentless drive to maximize accessible phase space under strict topological constraints.

Acknowledgments.—

The author gratefully acknowledges Rafik Ballou and Loren Coquille for their careful reading of the manuscript and valuable suggestions.

-
- [1] C. L. Henley, The “coulomb phase” in frustrated systems, *Annual Review of Condensed Matter Physics* **1**, 179 (2010).
- [2] W. Jockusch, J. Propp, and P. Shor, Random domino tilings and the arctic circle theorem (1998), [arXiv:math/9801068](https://arxiv.org/abs/math/9801068) [math.CO].
- [3] E. H. Lieb, Residual entropy of square ice, *Phys. Rev.* **162**, 162 (1967).
- [4] V. E. Korepin, Calculation of norms of bethe wave functions, *Commun. Math. Phys.* **86**, 391 (1982).
- [5] A. G. Izergin, Partition function of the six-vertex model in a finite volume, *Sov. Phys. Dokl.* **32**, 878 (1987), [Dokl. Akad. Nauk SSSR 297, 378 (1987)].
- [6] H. Cohn, R. Kenyon, and J. Propp, A variational principle for domino tilings, *J. Amer. Math. Soc.* **14**, 297 (2001).
- [7] R. Kenyon, A. Okounkov, and S. Sheffield, Dimers and amoebae, *Ann. Math.* **163**, 1019 (2006).
- [8] F. Colomo and A. G. Pronko, The arctic curve of the domain-wall six-vertex model, *J. Stat. Phys.* **138**, 662 (2010).
- [9] A. D. King, J. Coraux, B. Canals, and N. Rougemaille, Magnetic arctic circle in a square ice qubit lattice, *Phys. Rev. Lett.* **131**, 166701 (2023).
- [10] G. T. Barkema and M. E. J. Newman, Monte carlo simulation of ice models, *Phys. Rev. E* **57**, 1155 (1998).
- [11] G. Wulff, Zur frage der geschwindigkeit des wachstums und der auflösung der krystallflächen, *Z. Kristallogr.* **34**, 449 (1901).
- [12] R. L. Dobrushin, R. Kotecký, and S. B. Shlosman, *Wulff Construction: A Global Shape from Local Interaction*, Translations of Mathematical Monographs, Vol. 104 (American Mathematical Society, Providence, RI, 1992).
- [13] M. E. Brooks-Bartlett, S. T. Banks, L. D. C. Jaubert, A. Harman-Clarke, and P. C. W. Holdsworth, Magnetic interaction fragmentation and monopole fragmentation, *Phys. Rev. X* **4**, 011007 (2014).
- [14] L. Berchialla, G. M. Macauley, and L. J. Heyderman, Focus on three-dimensional artificial spin ice, *Applied Physics Letters* **125**, 220501 (2024).
- [15] B. J. Alder and T. E. Wainwright, Phase transition for a hard sphere system, *J. Chem. Phys.* **27**, 1208 (1957).
- [16] S. Asakura and F. Oosawa, On interaction between two bodies immersed in a solution of macromolecules, *J. Chem. Phys.* **22**, 1255 (1954).
- [17] M. E. Fisher and P.-G. de Gennes, Phénomènes aux parois dans un mélange binaire critique, *C. R. Seances Acad. Sci. Ser. B* **287**, 207 (1978).
- [18] C. Hertlein, L. Helden, A. Gambassi, S. Dietrich, and C. Bechinger, Direct measurement of critical casimir forces, *Nature* **451**, 172 (2008).